Supplement of Atmos. Meas. Tech., 15, 3859–3874, 2022
https://doi.org/10.5194/amt-15-3859-2022-supplement

Atmospheric Measurement Techniques
Open Access
EGU

Supplement of

Substantial organic impurities at the surface of synthetic ammonium sulfate particles

Junteng Wu et al.

Correspondence to: Junteng Wu (junteng.wu@univ-amu.fr) and Anne Monod (anne.monod@univ-amu.fr)

S1 Statistical studies using AS particles since 2000

Article number in total	Optical properties	Hygroscopicity	Phase transition	Chemical reaction
219	44	115	49	62

AS mark	Related article number
Sigma-Aldrich/Merck	43
Fisher Chemical/Fluka	21
Alfa Aesar	7
Beijing Chemical Reagent	2
Mallinckrodt Baker	2
EMD Millipore	2
Tianjin	1
Shanghai Chemical and Medical Corporation	1
Univar	1
wako pure chemical	1
Not mentioned	137
In total	219

S2 Reagents

Reagents	Mark and purity	Lot
Ammonium sulfate crystal	ACROS Organics from Fisher Chemical, 99.5%	A0408697
Ammonium sulfate crystal	Merck, EMSURE	AM1034817 833
Ammonium sulfate crystal	Merck suprapur, 99.9999%	B1675709
Liquid water	Milli-Q water, 18.2 MΩ cm, TOC < 2ppb	Laboratory product
Liquid water	Fisher Chemical, LC-MS Grade	2047076
Liquid Ethanol	Fisher Chemical, 99.8%	1922061
Hydrochloric acid	Fisher Chemical, Trace metal grade	4118060
Acetonitrile	Fisher Chemical, Optima© LC/MS grade	1924623
Methanol	Fisher Chemical, Optima© LC/MS grade	1737574

Most of the ammonium sulfate particles used in the laboratory are commercial. About 90% of ammonium sulfate is produced by 3 different processes: (1) as a byproduct caprolactam production, (2) from synthetic manufacture by combining anhydrous ammonia and sulfuric acid, and (3) as a coke oven byproduct by reacting the ammonia recovered from coke oven offgas with sulfuric acid. No detailed information is given about the potential organic compounds during these manufacture processes.

Ref: Ammonium Sulfate Manufacture: Background Information For Proposed Emission Standards, EPA-450/3-79-034a, U. S. Environmental Protection Agency, Research Triangle Park, NC, December 1979.

S3 Comparison between EXP P1 and EXP P8 :

The effect of the gas supplier (used for nebulizing the AS solution), was investigated by replacing compressed air (EXP P1) by pure N_2 (EXP P8)

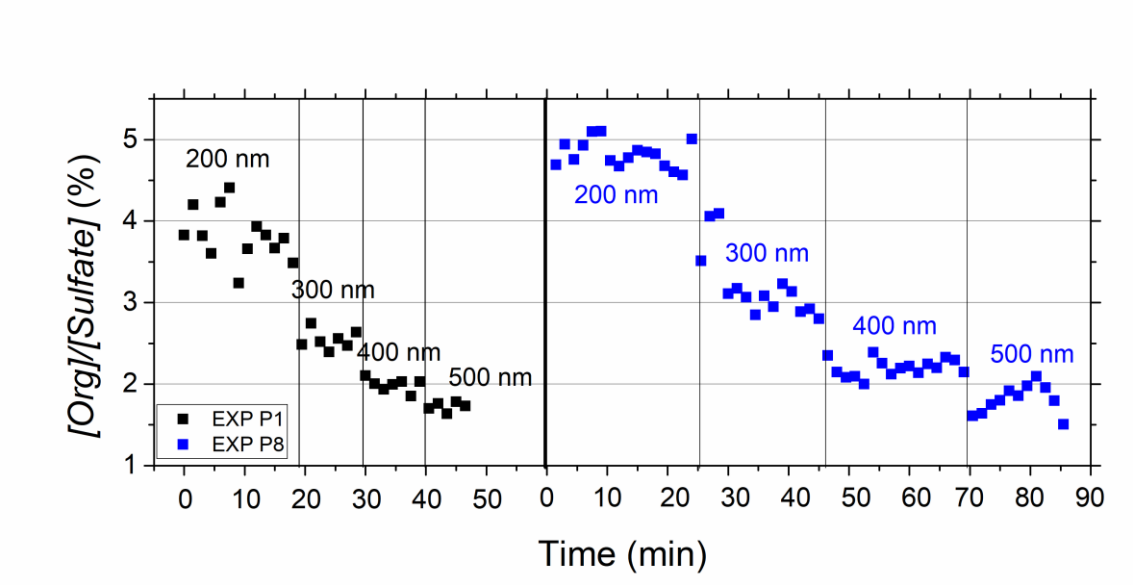

Figure S3: [Org]/[Sulfate] mass ratios obtained from the AMS measurements in EXP P1 using compressed air and in EXP P8 using pure N_2 (Linde Gas, 99.999 %). The AS concentration in the solution was the same for both experiments presented in this figure (0.5M).

S4 Investigating the AMS signals of NO_2^+ and NO+ fragments

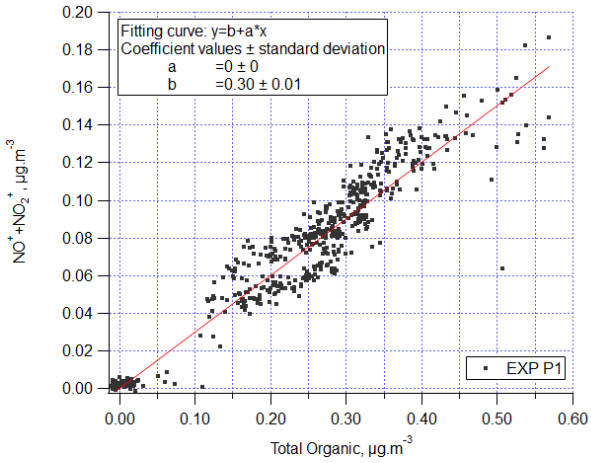

Figure S4-1: Linear plot of the AMS signals of the sum of NO_2^+ and NO^+ fragments (i.e. nitrate signal) versus the total organic signal during EXP P1.

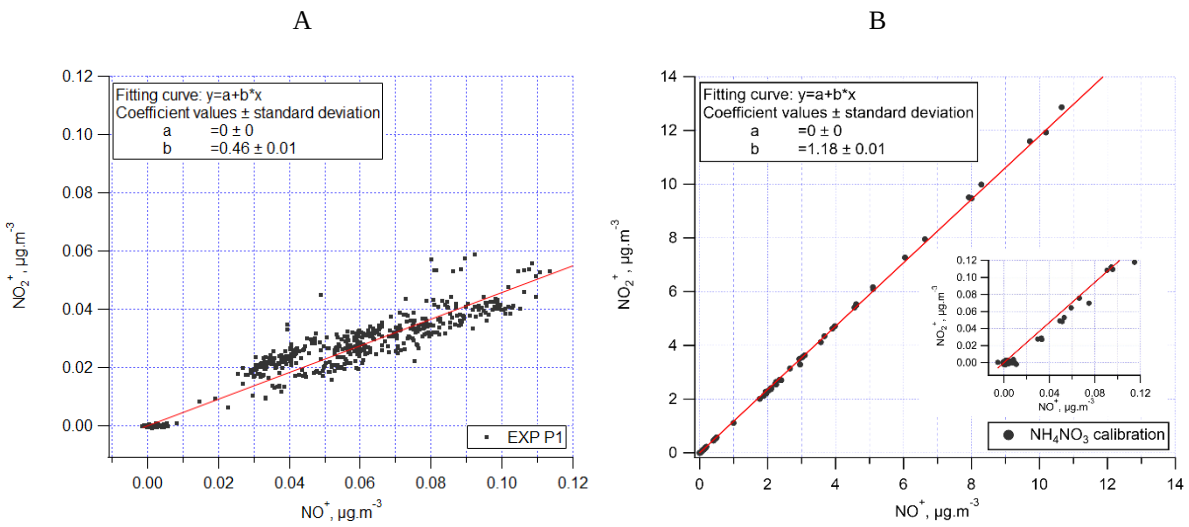

Figure S4-2: Linear plots of the AMS signals of NO_2^+ versus NO^+ fragments A) during EXP P1 and B) during the calibration using NH_4NO_3.

S5 Raw mass spectra of $C_xH_yN_x$ compounds (EXP P1 at AS concentrations of 0.5M)

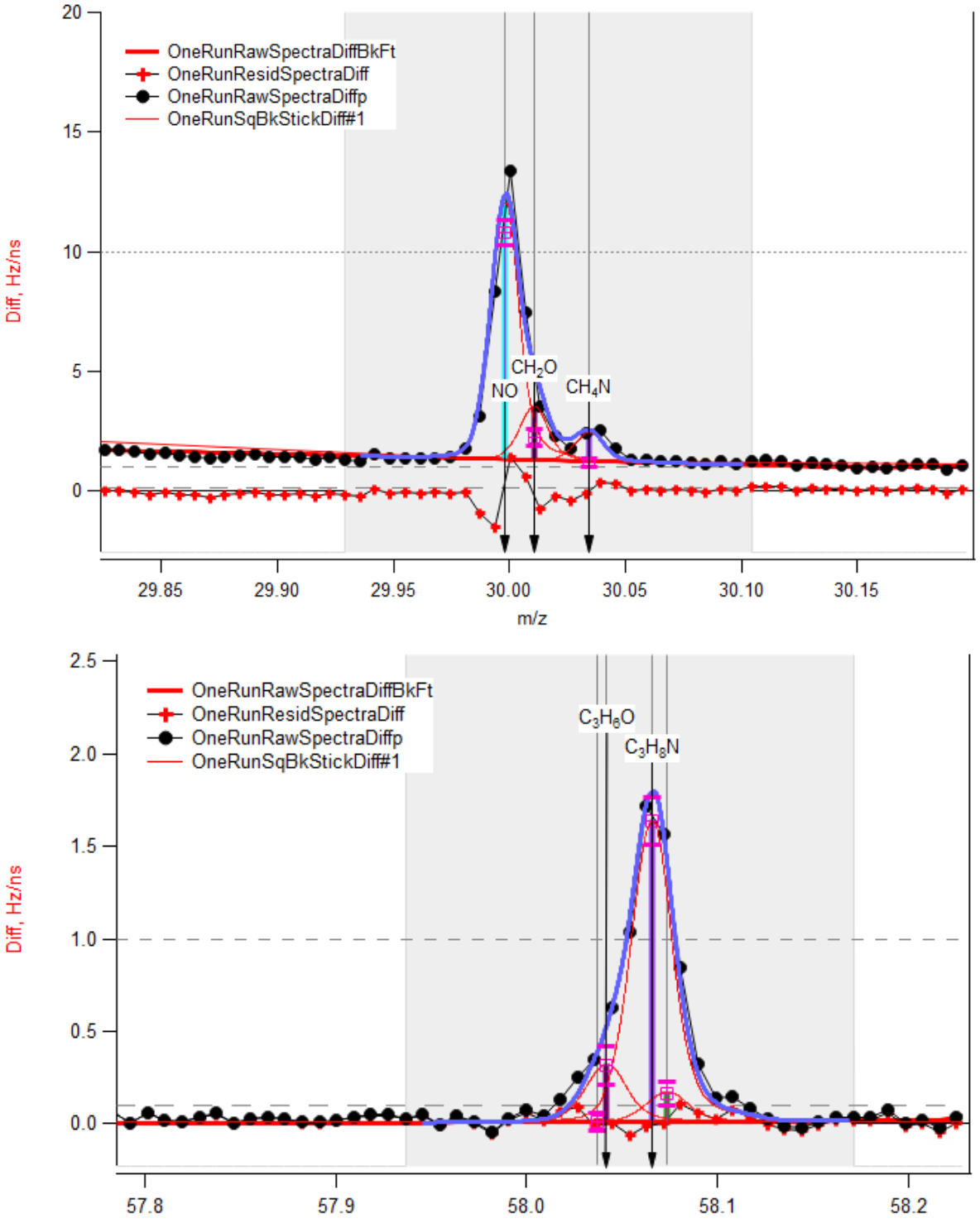

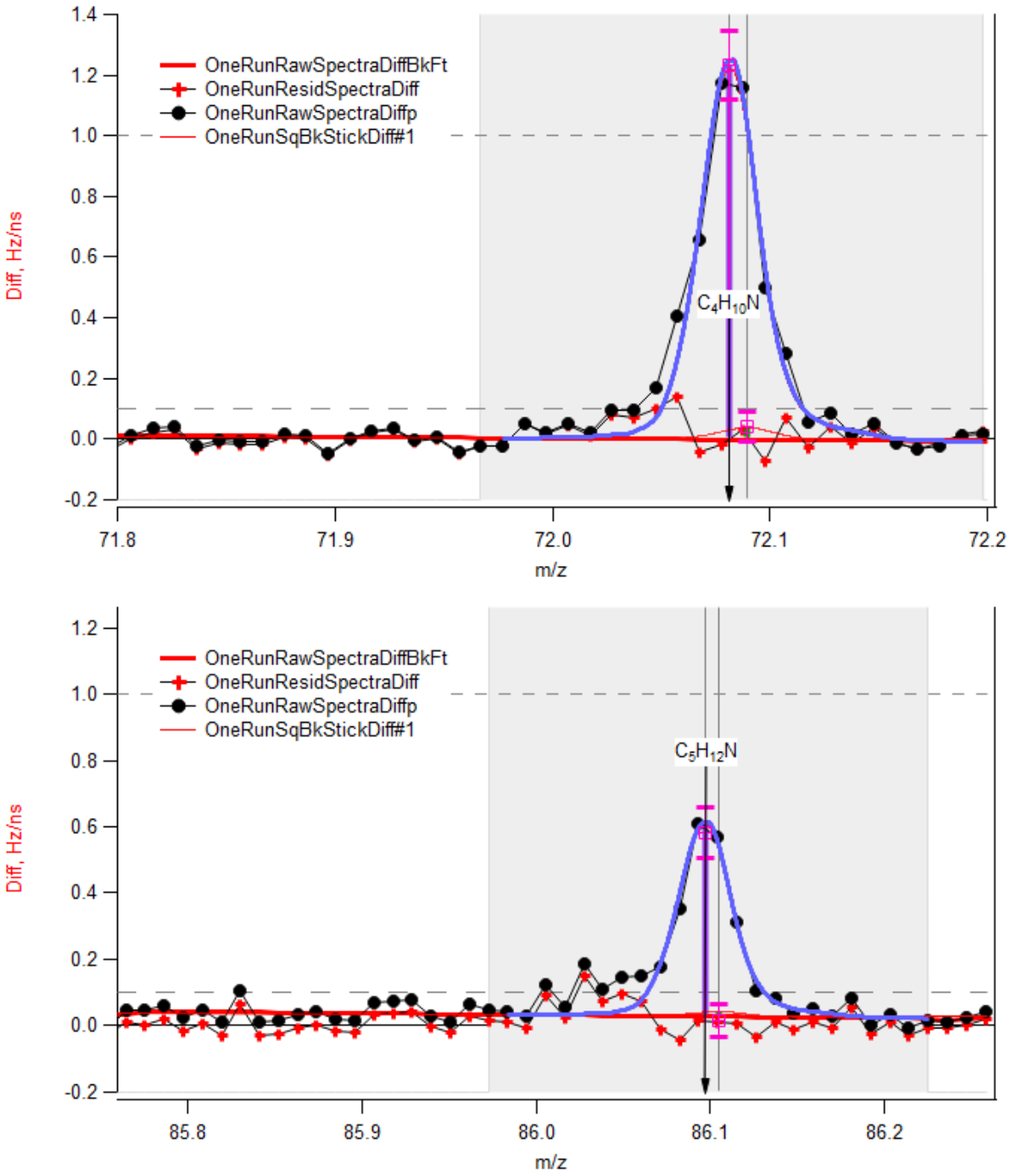

S6 Influence of the AAC rotational speed on the chemical content

To understand the influence of the rotational speed on the detection of organic traces, AS aerosols at d_a = 300 nm were selected in EXP P7 (Table 1) under three different rotational conditions: 190, 285 and 369 rad/s. In Figure S6: , the ratios of mass concentrations Org/Sulfate and $C_xH_yN_x$ /Sulfate are shown as a function of the rotational speed of the concentric cylinder in green and blue dots, respectively. Their averages are 2.9±0.1% and 0.48±0.04%. No significant difference has been observed with varying the rotational speed of AAC.

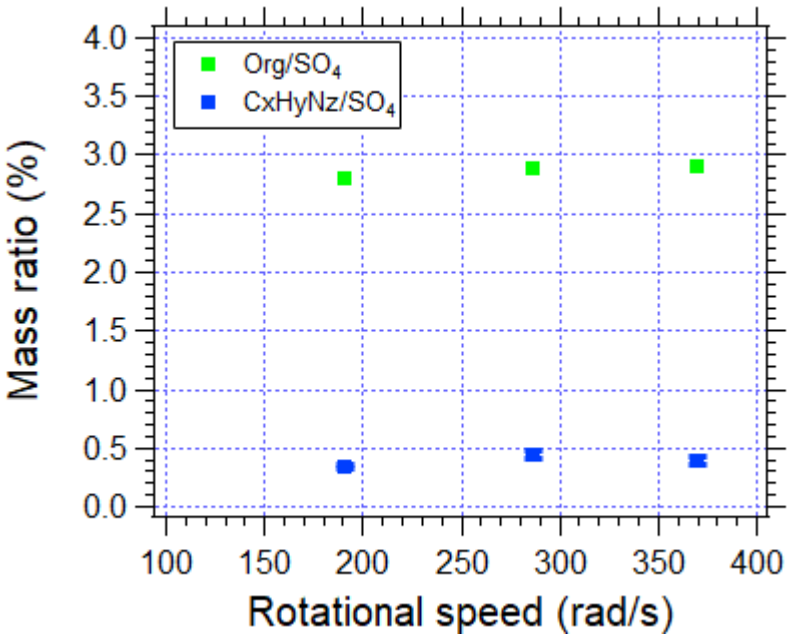

Figure S6: Effect of the AAC rotational speed on the organic content in AS particles (at da = 300 nm) measured by the HR-ToF-AMS (in EXP P7).

S7 Multi-charging corrections for the [Org]/[Sulfate] using the DMA for particle size selection

Under the hypothesis that organic compounds were coated homogenously on the surface of AS aerosol particles, the density was defined as $\rho_{org,S}$. The correction was done by removing the effects of multi-charged modes, so the corrected [Org]/[Sulfate] were represented only by the first mode. In a first step, [Org]/[Sulfate] were calculated using equation S5.1:

$$\frac{[Org]}{[Sulfate]}_{corr} = \frac{\sum_{1^{st}\,mode}(\pi d^2 N_d)\rho_{org,S}}{\sum_{1^{st}\,mode}\left(\frac{4}{3}\pi\frac{d^3}{2}\,N_d\right)\rho_{sulfate}} \qquad \text{Equation S7.1}$$

Where N_d is the number concentration at diameter d, $\sum_{1^{st}\,mode}(\pi d^2 N_d)$ is the total surface of all particles in the first mode measured by SMPS. $\sum_{1^{st}\,mode}\left(\frac{4}{3}\pi\frac{d^3}{2}\,N_d\right)$ is the total volume of all particles in the first mode. $\rho_{sulfate}$ is the volume density of sulfate in AS aerosols, 96.06 g.cm^{-3}.

Experimentally, [Org]/[Sulfate] mass concentration ratios were measured by the HR-ToF-AMS which considered all the particle sizes (including multi-charged modes) as described by equation SI7.2:

$$\frac{[Org]}{[Sulfate]}_{exp} = \frac{\sum_{d=0}^{\infty}(\pi d^2 N_d)\rho_{org,S}}{\sum_{d=0}^{\infty}\left(\frac{4}{3}\pi\frac{d^3}{2}\,N_d\right)\rho_{sulfate}} \qquad \text{Equation S7.2}$$

In the last step, combining Equation S7.1 and Equation S7.2, the corrected [Org]/[Sulfate] were obtained (equation S7.3), they gather the total amounts of organics and sulfate on the first DMA mode:

$$\frac{[Org]}{[Sulfate]}_{corr} = \frac{\sum_{1^{st}\,mode} N_d d^2}{\sum_{1^{st}\,mode} N_d d^3} \times \frac{\sum_{d=0}^{\infty} N_d d^3}{\sum_{d=0}^{\infty} N_d d^2} \times \frac{[Org]}{[Sulfate]}_{exp} \qquad \text{Equation S7.3}$$

Where all diameter information was recorded by the SMPS.

S8 Majors ions detected in LC/ESI+-MS of an aqueous solution of 1.5 M AS and their associated molecular formula and retention times.

m/z	Retention time	Proposed raw formula	Error (ppm)	DBE (double bond equivalence)
96.0813	3.00	$C_6H_{10}N$	0	2.0
113.1078	**2.44**	**$C_6H_{13}N_2$**	0.9	1.0
209.1655	3.00	$C_{12}H_{21}N_2O$	0.5	3.0
223.1450	2.73	$C_{12}H_{19}N_2O_2$	1.3	4.0
225.1600	**3.02 ; 3.36**	**$C_{10}H_{21}N_2O_2$**	**1.3**	3.0
226.1918	**2.89 ; 3.11**	**$C_{12}H_{24}N_3O$**	**0.4**	5.0
227.1762	**3.51**	**$C_{12}H_{23}N_2O_2$**	**0.9**	2.0
241.1553	2.73 ; 3.01	$C_{12}H_{21}N_2O_3$	0.4	3.0
245.1862	3.21	$C_{12}H_{25}N_2O_3$	1.2	1.0
269.0962	2.86 ; 3.93	$C_{12}H_{17}N_2O_3S$	0.7	5.0
303.1012	2.76 ; 3.08	$C_{12}H_{19}N_2O_5S$	1	4.0
306.1487	2.89	$C_{12}H_{24}N_3O_4S$	0.3	2.0
307.1328	3.00	$C_{12}H_{23}N_2O_5S$	0	2.0
321.1117	2.73	$C_{12}H_{21}N_2O_6S$	0.9	3.0
340.2599	**3.97**	**$C_{18}H_{34}N_3O_3$**	**0.3**	3.0
343.0997	2.72	$C_{11}H_{23}N_2O_6S_2$	0.3	1.0
349.0528	2.55 ; 3.12	$C_{12}H_{17}N_2O_6S_2$	0	5.0
420.2164	3.49	$C_{18}H_{34}N_3O_6S$	1	3.0
456.1835	3.25	$C_{17}H_{34}N_3O_7S_2$	0.7	2.0
533.3006	3.88	$C_{24}H_{45}N_4O_7S$	0.6	4.0

In this table, the bold m/z were studied in more details using LC/ESI$^+$-MS-MS (shown in S9).

S9 Comparison between experiments C9 and C10: LC/ESI+-MS base peak chromatogram of acetonitrile liquid-liquid extracts of aqueous AS solutions from ACROS Organics™ and EMSURE®,.

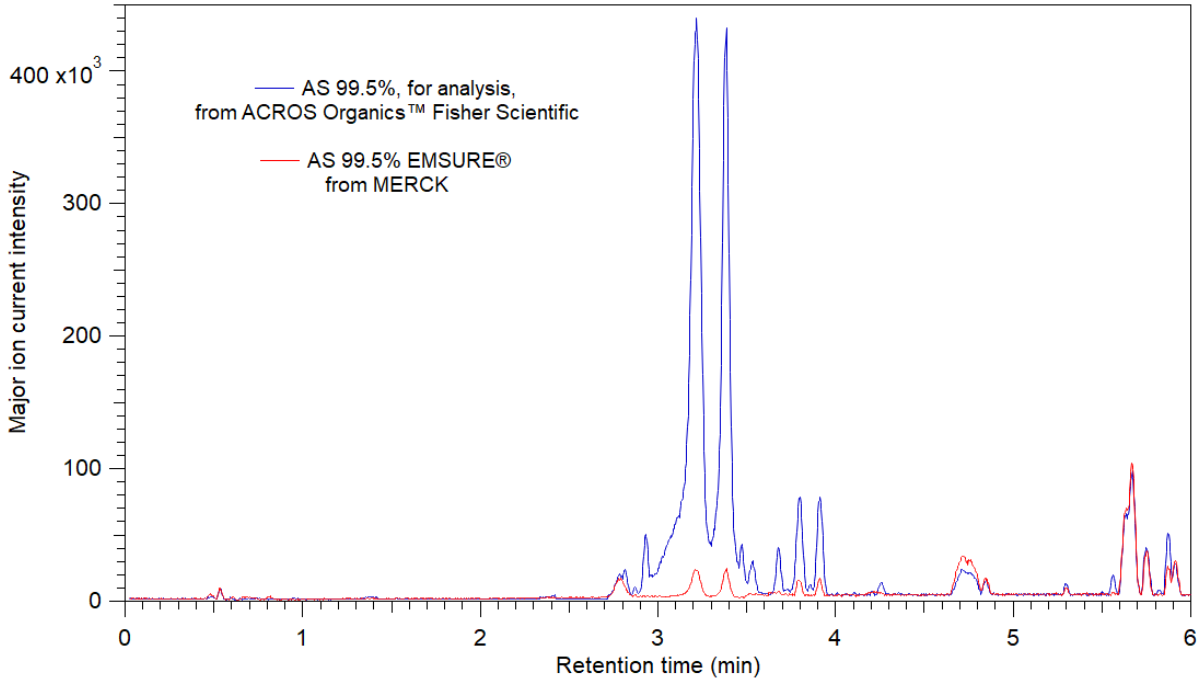

S10 LC/ESI+-MS-MS of the most intense ions found in the acetonitrile liquid-liquid extracts of aqueous AS solution and their fragments (experiment C9).

Precursor ion m/z	Fragment ions m/z
113.108	96.082 ; 81.059 ; 79.056 ; 69.072
225.160	125.107 ; 113.108 ; 96.082 ; 85.030 ; 79.056 ; 69.072
226.192	114.092 ; 113.108 ; 96.082 ; 79.056 ; 72.082 ; 69.072
227.177	113.108 ; 96.082 ; 79.056 ; 69.072
340.260	228.160 ; 132.103 ; 114.092 ; 96.082 ; 69.072

S11 Estimation of the error made on the critical supersaturation during the CCN activation of AS aerosol particles if one assumes 100% AS, omitting the presence of organic impurities This estimation is performed for AS aerosol particles (d_m = 130 nm) containing organic impurities with a mass fraction [Org]/[Sulfate] = 3.8 %. Considering ideal solutions, a simple calculation using the κ-Köhler equation (equation S11.1) from Petters and Kreidenweis, 2007, was performed.

$$SS = \frac{D^3 - d^3}{D^3 - d^3(1-\kappa)} \exp\left(\frac{4\sigma_{s/a} M_w}{RTD\rho_w}\right) - 100\% \qquad \text{Equation S11.1}$$

Where *SS* is the supersaturation, *D* and *d* are the droplet diameter and the particle diameter, respectively, κ is the hygroscopicity, $\sigma_{s/a}$ is the surface tension at the interface between droplet and air, M_w is the molar mass of water, *R* is the ideal gas constant, ρ_w is the density of water, and *T* is the temperature, fixed at 298.15 K.

For the estimation of *SS* in the presence of organic impurities, one needs to evaluate the values of effective kappa κ_{eff} and $\sigma_{s/a}$ on AS particles. To do so, two extreme hypotheses are explored for the organic fraction:

- **Hypothesis 1**: the organic fraction is considered non-surface-active with κ = 0.1. In this case, the surface tension is considered the same as pure water, i.e., 72 mN.m^{-1}; and the effective κ (κ_{eff}) is calculated following the ZSR (Zdanovskii, Stokes, and Robinson) assumption (Stokes and Robinson, 1966). With a mass fraction [Org]/[Sulfate] = 3.8%, the organic fraction in the particle, ε is 2.8%. And thus:

$$\kappa_{eff} = \varepsilon \times 0.1 + (1 - \varepsilon) \times 0.61 = 0.59$$

- **Hypothesis 2**: the organic fraction is considered as extremely surface-active using surfactin as the proxy for surfactant. In this case, κ is fixed at 0.61 and the surface tension varies according to the equilibrium surface tension isotherms of aqueous solutions of surfactin at various concentrations from Ekström et al., 2010 (Table S11).

Table S11: Simulation of the um surface tension isotherms of aqueous solutions of surfactin at various concentrations (Ekström et al., 2010).

Surfactin concentrations (mol.L^{-1})	$\boldsymbol{\sigma_{s/a}(mN.m^{-1})}$
$[\text{surfactin}] \leq 3 \times 10^{-6}$	28
$3 \times 10^{-6} < [\text{surfactin}] < 3 \times 10^{-5}$	$-19.1 \times \ln[\text{surfactin}] - 171$
$[\text{surfactin}] \geq 3 \times 10^{-5}$	72

Following hypothesis 1 and hypothesis 2, the supersaturation was calculated along the droplet activation, and the corresponding Köhler curves are shown in Figure S11 where the CCN activation curve of pure AS particles were added for comparison.

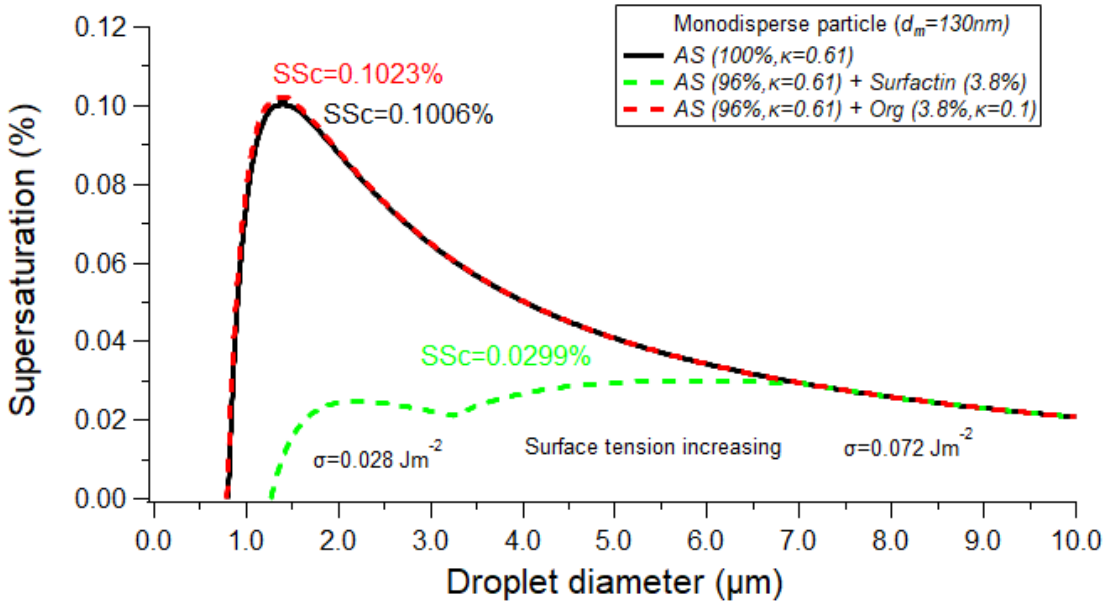

Figure S11: Calculated CCN activation curves of pure AS (solid black line), AS with non-surface-active organics using a mass ratio [Org]/[Sulfate] = 3.8% (dashed red line), and AS with extremely surface-active surfactin using a mass ratio [surfactin]/[Sulfate] = 3.8 % (dashed green line). SS_c is the critical supersaturation.

The results show that whereas the critical supersaturation is not significantly impacted by the presence of organic impurities under hypothesis 1, it is highly impacted under hypothesis 2, with a potential error of more than 70%.

S12 Investigation of the concentrations of organic surface-active species in an aqueous solution of AS

Organic surface-active species are amphiphile molecules, also called surfactants. Their potential presence in a concentrated 500 $g.L^{-1}$ solution of AS (Across 99.5 %) were quantified, following a method adapted from Nozière et al., 2017. This quantification method enables to differentiate surfactants by class, cationic, anionic, and non-ionic. Very low concentrations of surfactants were detected, as shown in Table S12. No anionic surfactants were detected. As the concentrations are below the quantification limit for cationic surfactants (65 nM) and for non-ionic surfactants (75 nM), these results should be interpreted with caution. Nevertheless, an upper limit of 140 nM for surfactants concentration was considered to investigate the implications of these results.

A concentration of 140 nM of surfactants in a 500 $g.L^{-1}$ AS solution is equivalent to a $[Org_{surfactant}]/[Sulfate]$ mass ratio of 1×10^{-5} %, taking cetyltrimethylammonium chloride (CTAC) as a standard for cationic surfactants and Triton X-100 as a standard for non-ionic surfactants. Because this ratio is 5 orders of magnitude lower than the total organic fraction detected in AS particles, it is likely that surfactants play a negligible role in organic impurities.

However, small concentrations of highly surface-active species can induce non-negligible effects on surface tension, and thus on CCN activity (Ovadnevaite et al., 2017; Nozière et al., 2017). We have thus investigated a rough estimation of the surface tension induced by the amount of surfactants observed. Considering AS particles with d_m = 130 nm (under our experimental conditions), the mass ratio of 1×10^{-5} % $[Org_{surfactant}]/[Sulfate]$ is equivalent to a concentration of 6×10^{-7} $mol.L^{-1}$ of surfactants. Note that this concentration is an upper value for the concentration of surfactants upon activation of the particles. For any surface-active molecule, the surface tension of a 6×10^{-7} $mol.L^{-1}$ solution is the same as that of pure water as shown by surface tension isotherms (see for example Fig. 3 in Ekström et al., 2010; Fig.2 in Frossard et al., 2019; or Fig. 2 in Arabadzhieva et al., 2020). It is thus concluded that the CCN activity of AS particles with d_m = 130 nm should not be affected by the presence of surfactants in AS crystals.

Table S14 Concentrations of surfactants by class in 10 mL of a 500 $g.L^{-1}$ solution of AS (ACROS 99.5 %). The quantification limits of cationic and non-ionic surfactants are shown in the table.

Surfactant type	**Cationic**	**Anionic**	**Non-ionic**
Concentration (nM)	< 65	Undetectable	< 75

References

Arabadzhieva, D., Tchoukov, P., and Mileva, E.: Impact of Adsorption Layer Properties on Drainage Behavior of Microscopic Foam Films: The Case of Cationic/Nonionic Surfactant Mixtures, Colloids Interfaces, 4, 53, https://doi.org/10.3390/colloids4040053, 2020.

Ekström, S., Nozière, B., Hultberg, M., Alsberg, T., Magnér, J., Nilsson, E. D., and Artaxo, P.: A possible role of ground-based microorganisms on cloud formation in the atmosphere, Biogeosciences, 7, 387–394, https://doi.org/10.5194/bg-7-387-2010, 2010.

Frossard, A. A., Gérard, V., Duplessis, P., Kinsey, J. D., Lu, X., Zhu, Y., Bisgrove, J., Maben, J. R., Long, M. S., Chang, R. Y.-W., Beaupré, S. R., Kieber, D. J., Keene, W. C., Nozière, B., and Cohen, R. C.: Properties of Seawater Surfactants Associated with Primary Marine Aerosol Particles Produced by Bursting Bubbles at a Model Air–Sea Interface, Environ. Sci. Technol., 53, 9407–9417, https://doi.org/10.1021/acs.est.9b02637, 2019.

Nozière, B., Gérard, V., Baduel, C., and Ferronato, C.: Extraction and Characterization of Surfactants from Atmospheric Aerosols, J. Vis. Exp. JoVE, https://doi.org/10.3791/55622, 2017.

Ovadnevaite, J., Zuend, A., Laaksonen, A., Sanchez, K. J., Roberts, G., Ceburnis, D., Decesari, S., Rinaldi, M., Hodas, N., Facchini, M. C., Seinfeld, J. H., and O' Dowd, C.: Surface tension prevails over solute effect in organic-influenced cloud droplet activation, Nature, 546, 637–641, https://doi.org/10.1038/nature22806, 2017.

Petters, M. D. and Kreidenweis, S. M.: A single parameter representation of hygroscopic growth and cloud condensation nucleus activity, Atmospheric Chem. Phys., 7, 1961–1971, https://doi.org/10.5194/acp-7-1961-2007, 2007.

Stokes, R. H. and Robinson, R. A.: Interactions in Aqueous Nonelectrolyte Solutions. I. Solute-Solvent Equilibria, J. Phys. Chem., 70, 2126–2131, https://doi.org/10.1021/j100879a010, 1966.